

Ultrahigh-temperature metamorphism of 2.0 Ga-Old sapphirine-bearing granulite from the Itabuna-Salvador-Curaçá Block, Bahia, Brazil

Metamorfismo de temperatura ultra-alta de granulitos com safirina de 2,0 Ga do Bloco Itabuna-Salvador-Curaçá, Bahia, Brasil

Johildo Salomão Figueiredo Barbosa¹, Angela Beatriz de Menezes Leal¹, Reinhardt Adolfo Fuck²,
Jailma Santos de Souza de Oliveira¹, Philippe Gonçalves³ and Carlson de Matos Maia Leite¹

¹Universidade Federal da Bahia – UFBA, Instituto de Geociências, Departamento de Geologia, Pós-graduação em Geologia,
Rua Barão de Geremoabo, s/n, Salvador, BA, Brasil (johildo.barbosa@gmail.com; angelab@ufba.br;
jailmasouza@gmail.com; carlson.leite@gmail.com)

²Universidade de Brasília – UnB, Instituto de Geociências, Brasília, DF, Brasil (reinhardt@unb.br)

³Université Blaise Pascal France, Laboratoire Magmas et Volcans – LMV, Clermont-Ferrand, France
(philippe.gonçalves@uni-fcomte.fr)

Recebido em 22 de maio de 2015; aceito em 2 de setembro de 2016

Abstract

The study area is located in the São Francisco Craton, in the southern part of the State of Bahia, Brazil. In this region, the Palaeoproterozoic Itabuna-Salvador-Curaçá Block (ISCB) comprises supracrustal rocks associated with tonalite/trondhjemite and monzonite orthogneisses together with subordinate metamafic rocks of Archean and Palaeoproterozoic ages. All exposed rocks are strongly deformed and were re-equilibrated under granulite facies conditions at 2.07-2.08 Ga. The supracrustal rocks include a sapphirine-bearing granulite that contains sapphirine, quartz, orthopyroxene, sillimanite, garnet, mesoperthite, plagioclase, biotite and cordierite. Based on microstructural relations, the metamorphic peak paragenesis of the sapphirine-bearing granulite is $Grt_1 + Opx_1 + Bt_1 + Qtz + Sil_1 + Spr_1 + Mp$. Mineral reaction microstructures, such as symplectitic coronas around porphyroblasts, helped to identify the following retrograde parageneses, interpreted as formed during the tectonic rise of these rocks: $Grt_1 \pm Qtz = Opx_2 + Sil_2$, $Grt_1 = Opx_2 + Spr_2 (+ Sil_2)$, $Opx_1 + Sil_1 + Qtz = Crd$ and $Grt_1 + Qtz = Opx_3 + Crd$. In turn, $Bt_2 + Qtz$ symplectites formed by the reaction $Opx_{1,2} + Mp + H_2O = Bt_2 + Qtz$ record the retrograde cooling path. Thermobarometry calculations were performed by means of the multiequilibria method (e.g. THERMOCALC) and classic thermobarometers, which indicated $P = 7-11$ kbar and $T = 900$ °C for the sapphirine-bearing granulite. One of the mechanisms associated with the ultrahigh-temperature metamorphism is the addition of radioactive material and the presence of basaltic magmas during the formation of ISBC. Fractional crystallization of basaltic magma produced tonalite intrusions, dated approximately 2.15-2.13 Ga, close to the metamorphic peak at 2.07-2.08 Ga.

Keywords: Sapphirine-bearing granulite; Geothermobarometry; Palaeoproterozoic; Itabuna-Salvador-Curaçá block.

Resumo

A área de pesquisa se situa no Cráton do São Francisco, no sul da Bahia, Brasil. Nessa região, no segmento crustal Bloco Itabuna-Salvador-Curaçá (BISC), ocorrem rochas supracrustais associadas a gnaisses tonalíticos/trondhjemíticos a monzoníticos e rochas maficas subordinadas, de idades arqueana e paleoproterozoica, todos fortemente deformados e reequilibrados na fácie granulito em 2,07 a 2,08 Ga. As rochas supracrustais incluem granulitos com safirina constituídos por quartzo, ortopiroxênio, sillimanita, granada, mesoperftita, plagioclásio, biotita e cordierita. Com base nos arranjos microestruturais entre os minerais constituintes dos granulitos com safirina, a paragênese de pico metamórfico é $Grt_1 + Opx_1 + Bt_1 + Qtz + Sil_1 + Spr_1 + Mp$. Microestruturas de reações entre minerais, como coroas de simpleteitos ao redor de porfiroblastos, permitiram identificar as seguintes paragêneses retrógradas, interpretadas como formadas durante a ascensão tectônica dessas rochas: $Grt_1 \pm Qtz = Opx_2 + Sil_2$, $Grt_1 = Opx_2 + Spr_2 (+ Sil_2)$; $Opx_1 + Sil_1 + Qtz = Crd$ e $Grt_1 + Qtz = Opx_3 + Crd$. Por sua vez, simpleteitos de $Bt_2 + Qtz$ formados pela reação $Opx_{1,2} + Mp + H_2O = Bt_2 + Qtz$ estão relacionados à evolução retrógrada durante resfriamento. Cálculos termobarométricos realizados com aplicação de termobarômetros clássicos e método

de multiequilíbrios (THERMOCALC, por exemplo) indicaram $P = 7\text{--}11$ kbar e $T \geq 900^\circ\text{C}$ para os granulitos com safirina. Um dos mecanismos associados à elevada temperatura está relacionado à adição de material radioativo com a presença de magmas basálticos durante a formação do BISC. A cristalização fracionada desses magmas produziu intrusões tonalíticas que datam de aproximadamente de 2,15 a 2,13 Ga, próximo do pico do metamorfismo de 2,07 a 2,08 Ga.

Palavras-chave: Granulito com safirina; Geotermobarometria; Palaeoproterozoico; Bloco Itabuna-Salvador-Curaçá.

INTRODUCTION

The Paleoproterozoic Itabuna-Salvador-Curaçá Block (ISCB) is a large metamorphic province composed of amphibolite- and granulite-facies rocks that were formed during continent-continent collision (Barbosa and Sabaté, 2002, 2004). It is located in eastern Brazil and constitutes part of the São Francisco Craton (Almeida, 1977), one of the most important geotectonic units of South America (Cordani et al., 1992; Alkmim et al., 1993; Teixeira et al., 1996; Oliveira et al., 2010). Detailed investigations of this terrain started with petrochemical and mineralogical studies, which were undertaken mainly with the purpose of investigating the metallogenetic potential of the area (Barbosa, 1986, 1990; Barbosa and Fonteilles, 1989; Barbosa, 1996; Iyer et al., 1995; Figueiredo, 1989; Figueiredo and Barbosa, 1993; Marinho et al., 1992; Aillon, 1992; Fornari, 1992; Ledru et al., 1994; Alves da Silva et al., 1996; Leite, 2002; Peucat et al., 2011; Souza-Oliveira et al., 2014). These studies revealed the composition of the metamorphic products and the tectonic setting of their protoliths, together with their crystallization ages and the pressure and temperature conditions that prevailed during metamorphism. Pressures of 7–8 kbar and temperatures of 800–850 °C (Barbosa, 1986; Barbosa and Fonteilles, 1989) were obtained, in agreement with the expected metamorphic evolution of the granulitic terranes (Bohlen, 1987). Nevertheless, in some places temperatures of about 1000 °C are recorded in sapphirine-bearing granulites (Leite, 2002; Pinho, 2005; Leite et al., 2009) pointing to UltraHigh-Temperature (UHT) conditions (Harley, 1998).

Sapphirine-bearing granulites have been reported in high-grade terranes in Antarctica (e.g., Ellis, 1980; Grew, 1980; Dallwitz, 1986; Motoyoshi and Hensen, 2001; Iwamura et al., 2013), Canada (e.g., Morse and Talley, 1971; Arima and Grower, 1991), the Limpopo Belt (e.g., Harris and Holland, 1984; Perchuk, 2011; Tsunogae and Van Reenen, 2011), Madagascar (e.g., Nicollet, 1990; Gonçalves et al., 2004), the Eastern Ghats Belt, India (e.g., Grew, 1982; Dasgupta et al., 1995; Nasipuri et al., 2009) and the Brasília Belt, central Brazil (Moraes et al., 2002; Baldwin et al., 2005). The occurrence of this rock type is relevant to the reconstruction of the metamorphic history and the geotectonic evolution of these terranes, because they preserve a variety of prograde- and retrograde-related microstructures formed at extreme thermal conditions (Kienast and Ouzegane, 1987).

In this paper, our main goal is to present microstructures and mineral compositions for sapphirine-garnet-orthopyroxene-sillimanite-quartz-bearing granulites that occur in the southern part of ISCB (Leite et al., 2009). From the mineral chemistry data, the evolution of UHT metamorphism will be discussed and the P-T-time path will be characterized in order to understand the tectonic setting in which such extreme conditions were reached (e.g. Kelsey and Hand, 2015).

REGIONAL GEOLOGY

The study area is located in the São Francisco Craton, State of Bahia, Brazil. The craton is surrounded by Neoproterozoic fold and thrust belts formed during the Brasiliano/Pan-African orogeny at *ca.* 700–550 Ma (Caby et al., 1981) (Figure 1A). The largest basement exposures occur in Bahia (Figure 1B) where they comprise: (i) Archaean-Paleoproterozoic, medium to high-grade metamorphic rocks and remnants of greenstone belts and volcano-sedimentary sequences, intruded by Palaeoproterozoic granites, syenites and to a lesser extent mafic-ultramafic bodies; and (ii) Paleo-Mesoproterozoic (mainly siliciclastic sediments) and Neoproterozoic (mainly carbonate sediments) covers (Barbosa and Dominguez, 1996; Barbosa et al., 2012). The main litho-geotectonic units recognized within this basement are described below (Figure 1B).

The Gavião Block is composed of orthogneisses and migmatites, with amphibolite bodies dating *ca.* 2.7–3.2 Ga (Mougeot, 1996; Peucat et al., 2002). The block includes an older core of a 3.4 to 3.2 Ga trondhjemite-tonalite-granodiorite (TTG) suite (Martin et al., 1991; Santos Pinto, 1996). Within the Gavião Block, 3.2 to 2.9 Ga greenstone belts also occur (Marinho, 1991; Cunha et al., 1996; Bastos Leal, 1998; Peucat et al., 2002; Barbosa et al., 2012; Cunha et al., 2012; Menezes Leal et al., 2015). They were equilibrated at the greenschist facies and comprise komatiites with spinifex texture passing upwards to mafic and felsic volcanic rocks with intercalations of pyroclastic rocks and siliciclastic sediments (Marinho, 1991; Cunha and Fróes, 1994; Mascarenhas and Silva, 1994).

The 3.2 to 2.9 Ga Serrinha Block is composed of banded gneisses, amphibolites and mainly a granodiorite gneiss, mostly metamorphosed to the amphibolite facies (Silva, 1996; Rios, 2002). 2.2–2.1 Ga Paleoproterozoic greenstone belts also compose this block (Silva, 1992, 1996).

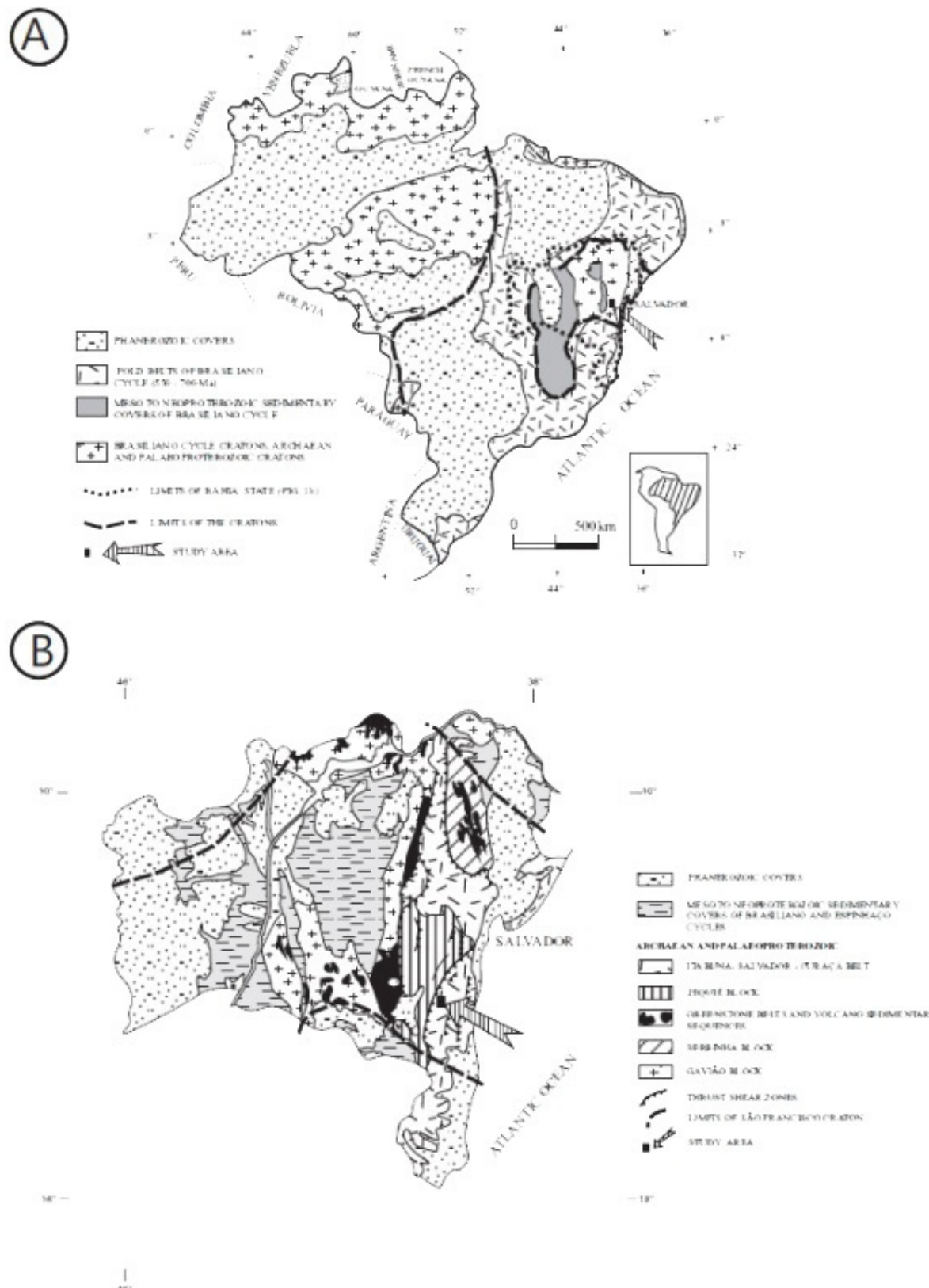


Figure 1. (A) Cratons and fold belts of the Brasiliano Cycle (Almeida et al., 1976; Almeida, 1977) after Schobbenhaus et al. (1984); (B) Geotectonic domains in Bahia (simplified from Barbosa and Dominguez, 1996) with location of the study area.

The Jequié Block (Cordani, 1973; Barbosa, 1986, 1990; Barbosa and Sabaté, 2002, 2004) is mainly formed of 2.7-2.6 Ga enderbitic and charnockitic granulites (Alibert and Barbosa, 1992), and migmatitic and heterogeneous granulites (charnockites with intercalations of mafic and felsic granulitic bands) with ages of 3.2 Ga (Marinho et al., 1992). In the heterogeneous granulites, granulitized supracrustal rocks, including mafic and felsic metavolcanic rocks, quartzites, iron formations and aluminous-magnesian granulites, are present and are occasionally crosscut by anatetic garnet- and cordierite-bearing granites (Barbosa and Sabaté, 2002, 2004; Pinho, 2005; Leite, 2002; Leite et al., 2009).

The segment of the Itabuna-Salvador-Curaçá Block (ISCB) is mainly composed of tonalitic and charnockitic orthogneisses with mafic-ultramafic enclaves and less abundant supracrustal rocks equilibrated to the granulite facies (Barbosa, 1986, 1990; Barbosa and Sabaté, 2002; Leite, 2002). The protoliths of the ISCB segment are volcanic and/or plutonic rocks of shoshonitic, low K-calc-alkaline and tholeiitic affinities with ages from 2.6 to 2.4 Ga (Ledru et al., 1994). The tectonic setting and geochemical characteristics of these rocks resemble those of recent volcanic arcs, such as Japan (Barbosa, 1990), or the active Chilean continental margin (Figueiredo, 1989).

The Gavião, Serrinha and Jequié blocks collided to form ISCB (Barbosa and Sabaté, 2002, 2004). These were deformed by at least three phases of ductile deformation. The first phase (F1) is characterized by large tight folds with sub-horizontal axial planes that verge westwards (Figure 2). The second phase (F2) produced open folds coaxial to the first ones in the Jequié Block, and tight folds in the Itabuna segment with a pronounced vertical axial plane foliation (Figure 2). The third deformation phase (F3), well developed in the ISCB segment, is represented by NE-SW trending vertical sinistral transpressional shear zones and sub-vertical foliation (Figure 2). All these deformation phases are coeval with granulite facies metamorphism dated at 2.07-2.08 Ga (Ledru et al., 1994; Pinho, 2005; Silva et al., 2002).

The P-T conditions of the high-grade metamorphism in the ISCB segment were studied by Barbosa (1986) and Barbosa and Fonteilles (1991). Based on garnet-bearing basic granulites from scarce outcrops, these authors obtained pressure estimates close to 7 kbar and temperatures in the range of 850 and 870 °C. The sapphirine-bearing granulites dispersed in this segment were previously mentioned by Silva (1991) and Seixas (1993).

GEOLOGICAL SETTING

The sapphirine-bearing granulite of this study occurs within a band of supracrustal rocks, tectonically imbricated in tonalite orthogneisses of the ISCB segment (Figure 2). The high-grade supracrustal rocks are exposed as lenses

along a subvertical to vertical shear zone related to F3 (Figure 2). A stretching lineation, defined by orthopyroxene orientation, plunges 5-15° to the northeast. Rootless folds are interpreted as preserved structures from F1 and F2 (Figure 2). Northwest of the study area, interference patterns that were formed during the first two deformation phases in the tonalitic orthogneiss (Figure 2) are correlated with the beginning of the collision (Barbosa and Sabaté, 2002, 2004).

The granulitic supracrustal rock of the ISCB segment contains the following interbanded rock types (Figure 2): (i) quartz-feldspathic granulite (1-100m wide); (ii) mafic granulite (1-50 m wide); (iii) iron-manganese formations (0.50-20 m wide); (iv) quartzite (10-250 m wide); (v) calc-silicate rocks, marble and pyroxenite (0.50-40 m wide); and (vi) sapphirine-bearing granulite (0.20-30 m wide).

The quartz-feldspathic and mafic granulites are predominant. The quartz-feldspathic layers are in general of medium grain size (5 mm-1.5 cm) and composed of quartz, mesoperthite, plagioclase and rare orthopyroxene. Ilmenite is the most common accessory phase, while green hornblende and biotite, always in coronas around orthopyroxene, are secondary. The mafic granulite is a fine- to medium-grained rock (1-5 mm) composed of plagioclase, orthopyroxene and clinopyroxene. The mafic granulites are probably metamorphosed tholeiitic volcanics (Barbosa, 1986, 1990). The iron formations are composed of ilmenite/magnetite and quartz; manganese layers are always superficially weathered and composed of pyrolusite and psilomelane. Small quantities of plagioclase, mesoperthite, clinopyroxene and opaque minerals are present in the quartzites. Calcite, plagioclase and clinopyroxene are the main constituents of calc-silicate rocks and marbles. Pyroxenes, hornblende, opaque minerals and minor plagioclase are present in the pyroxenites, which are sometimes intercalated with the supracrustal rocks.

The sapphirine-bearing granulite lenses (200m-20 km long and 15-50 m wide) are rare and occur in contact with the quartz-feldspathic and mafic granulitic rocks. They are mainly composed of sapphirine, quartz, orthopyroxene, sillimanite, garnet, mesoperthite, plagioclase, biotite and cordierite. In some of the outcrops, parallel undeformed leucosome veins are observed in rocks. They also can be observed when cross-cutting it in layers. The leucosomes contain mesoperthite, plagioclase, quartz, garnet, biotite and rarely orthopyroxene, cordierite and opaque minerals. It is believed that they have been formed in the metamorphic peak, after the ductile deformation phases (F1, F2, F3) (Barbosa, 1986, 1990; Seixas, 1993).

The tonalitic orthogneiss layers vary in thickness (1 cm-5 m), the lighter layers being composed of quartz and plagioclase, while the darker greenish-grey layers also contain orthopyroxene and opaque minerals. Garnet is dispersed throughout the rock. The rock is medium-grained (5 mm-1 cm) with blastomylonitic texture. Strong deformation

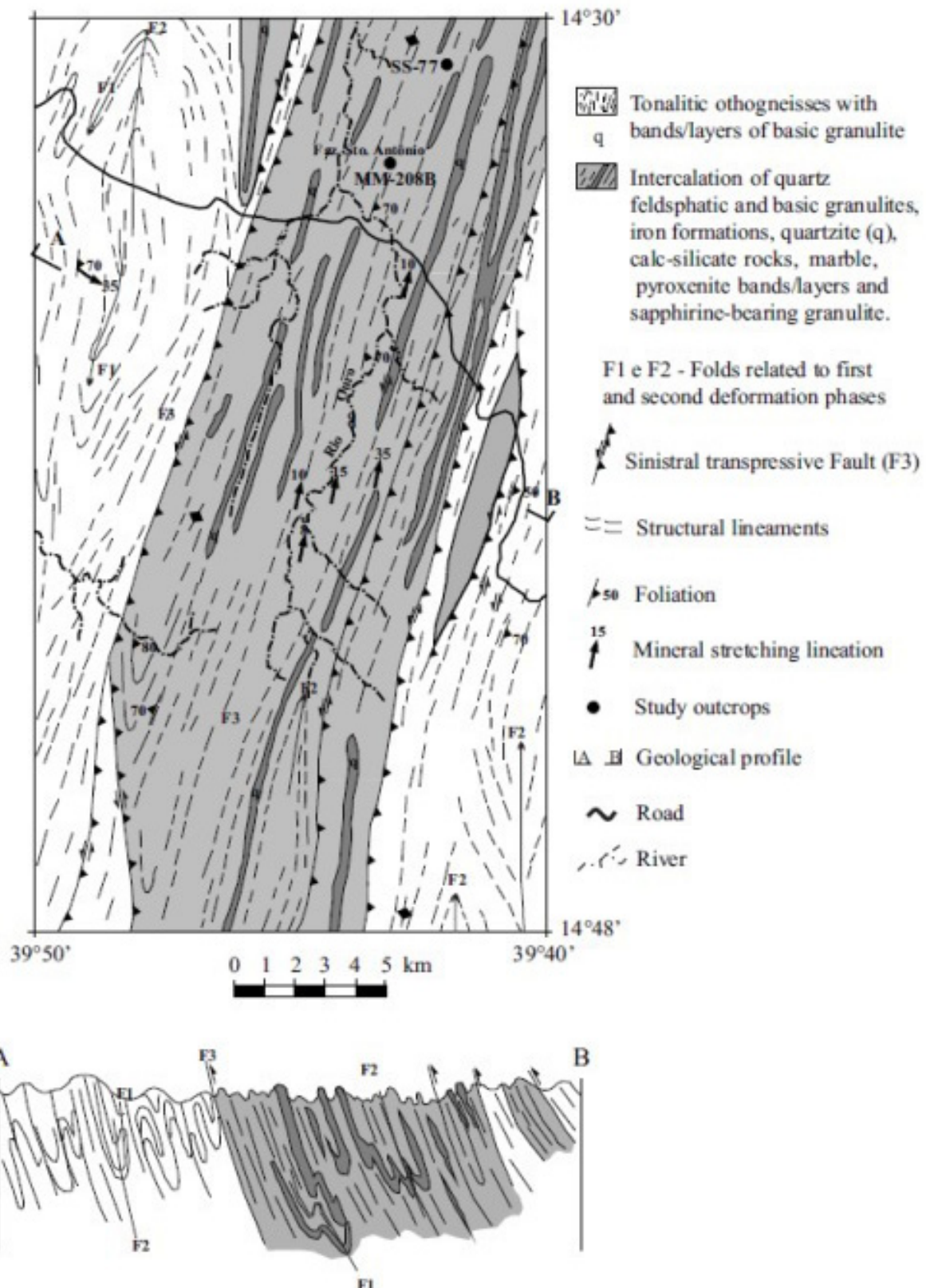


Figure 2. Simplified geological map and section of the ISCB segment with supracrustal granulitized rocks and their host tonalitic orthogneiss.

and recrystallization under granulite facies conditions make the distinction between volcanic and plutonic protoliths difficult. However, some outcrops show deformed feldspar porphyroclasts within a fine-grained recrystallized matrix, suggesting that the intrusive rocks were reequilibrated under granulite facies with metamorphic conditions (Barbosa, 1986, 1990). Rock-forming minerals are quartz and plagioclase. Garnet and orthopyroxene are scarce. The composition of the plagioclase (oligoclase) and whole rock geochemistry suggest that these rocks comprise metamorphosed (low-K calc-alkaline) tonalites (Barbosa, 1986).

In only a few outcrops the contact between the high-grade supracrustal rocks and the tonalite orthogneiss is exposed. It is as sharp as the other tectonic contacts observed between quartz-feldspathic layers, mafic granulite, iron-manganese formations, quartzites, calc-silicate rocks, marble and pyroxenite. These units are separated by sinistral shear zones formed during F3 (Figure 2).

PETROGRAPHY AND MINERAL REACTIONS

We studied the most representative outcrops of the sapphirine-bearing granulite (MM-208-B and SS-77 samples) (Figure 2). Their petrography, microstructures and mineralogical assemblages are described below.

The near-peak metamorphic assemblage is made of garnet (Grt_1), orthopyroxene (Opx_1), sillimanite (Sil_1), biotite (Bt_1), quartz or sapphirine (Spr_1), plagioclase (Pl_1) and mesoperthite (Mp_1). The main mineral phases are in contact with each other. Contacts between quartz and sapphirine have not been observed.

Among the metamorphic peak minerals, garnet (Grt_1) is usually present as 0.3-1.5 cm anhedral, rarely euhedral porphyroblasts, and commonly includes quartz and biotite. Orthopyroxene (Opx_1) occurs as 0.2-1.0 cm porphyroblasts with biotite, quartz and opaque inclusions. The Opx_1 grains are sometimes stretched, defining a mineral lineation. Sillimanite (Sil_1) appears as elongated prismatic crystals in the matrix, which are oriented parallel to the foliation. In some cases, sillimanite forms inclusions within orthopyroxene and mesoperthite. Biotite (Bt_1) is present as inclusions in garnet and orthopyroxene, or as large crystals in the matrix. Sometimes (especially in leucosome veins samples) it has polygonal contacts (Figure 3A). Sapphirine (Spr_1) is rare and occurs as small (0.1-0.5 mm) inclusions in contact with rutile (Rt), orthopyroxene (Opx_1) (Figure 3B) and garnet (Grt_1). Minor mesoperthite and plagioclase (Pl) are present in the matrix. Quartz occurs within garnet and in the matrix, where it forms platy crystals parallel to the foliation.

The most common accessory phase is dark-brown euhedral rutile, which is also presented as inclusions within quartz and orthopyroxene porphyroblasts (Figure 3B). Ilmenite,

magnetite, monazite, zircon and graphite occur in the matrix or as small inclusions within the main mineral phases.

Symplectitic and moat microstructure

Symplectites developed between porphyroblasts provide evidence for the retrograde reactions, which occurred in the sapphirine-bearing granulite. Coarse symplectitic intergrowths composed of orthopyroxene (Opx_2) and sillimanite (Sil_2) separate garnet and quartz (Figure 3C). These symplectites could have been formed according to the divariant FMAS reaction (e.g., Kriegsman, 1996):



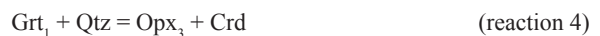
A second generation of sapphirine (Spr_2) is observed in symplectitic intergrowth with orthopyroxene (Opx_2) and sometimes with sillimanite (Sil_2), resorbing large garnet crystals (Grt_1) (Figure 3D). This type of symplectite is found only at the rims of orthopyroxene porphyroblasts in contact with garnet. This microstructure suggests the following (dis)continuous FMAS reaction:



Cordierite (Crd) moats, sometimes altered to pinnite, occur around orthopyroxene. Some of these moats have sillimanite and quartz inclusions. We infer that cordierite was formed by the univariant FMAS reaction:



Symplectites of cordierite with blebby orthopyroxene (Opx_3) replace garnet in the presence of quartz (Figure 3E). This microstructure could have been produced by the divariant FMAS reaction:



A second generation of biotite (Bt_2) forms intergrowths with quartz (Figure 3F), close to orthopyroxene when in contact with mesoperthite, according to the continuous KFMASH reaction:



MINERAL CHEMISTRY

Analytical procedure

Mineral compositions were obtained using the Camebax SX-50 electron microprobe at Paris VI University. Operating conditions were 15 kV accelerating voltage and 10 nA sample

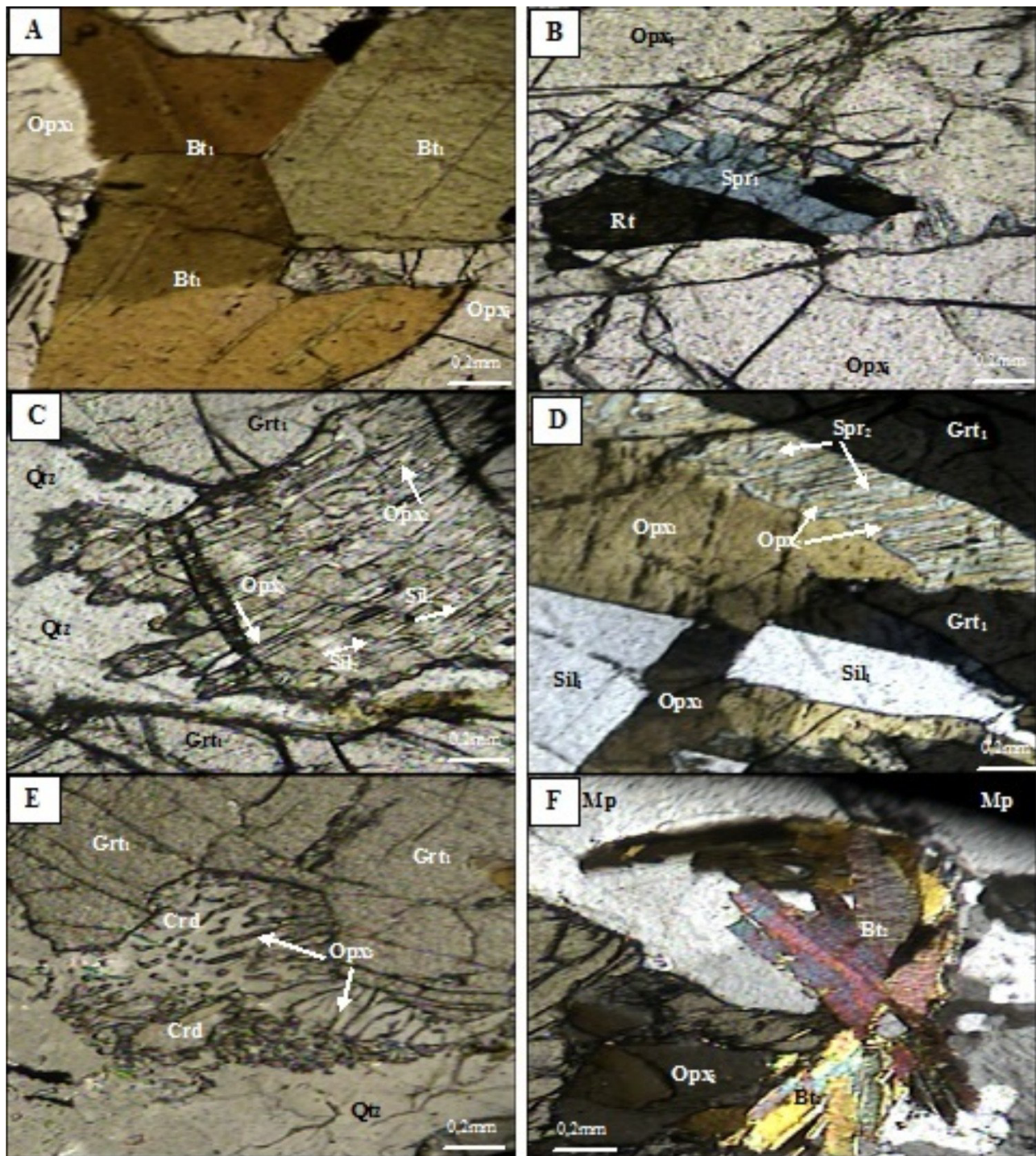


Figure 3. Photomicrographs of minerals and microstructures. (A) Biotite (Bt_1) with polygonal faces in the leucosome vein, sample MM-208B, plane-polarized light (ppl); (B) Sapphirine (Spr_1) and rutile (Rt) inclusions in orthopyroxene porphyroblast (Opx_1), sample MM-208B, ppl; (C) Silimanite (Sil_2)-orthopyroxene (Opx_2) symplectite against garnet and quartz that is interpreted to reaction (1) $Grt_1 + Qtz = Opx_2 + Sil_2$, sample MM-208B, ppl; (D) Sapphirine (Spr_2) – orthopyroxene (Opx_2) at the rims of orthopyroxene (Opx_1) porphyroblast in contact with garnet (Grt_1) demonstrating reaction (2) $Opx_1 + Grt_1 = Opx_2 + Spr_2$, sample MM-208B, ppl; (E) Orthopyroxene (Opx_3) – cordierite symplectite between garnet (Grt_1) and quartz recording reaction (4) $Grt_1 + Qtz = Opx_3 + Crd$, sample SS-77, ppl; (F) Biotite (Bt_2) – quartz intergrowth against orthopyroxene (Opx_{1-2}) and mesoperthite crystals suggesting reaction (5) $Opx_{1-2} + Mp + H_2O = Bt_2 + Qtz$, sample MM-208B, ppl.

current. Natural silicates and synthetic oxides were used as standards for all elements. Representative mineral phase analyses are shown in Tables 1-6. Structural formulas (garnet, orthopyroxene, biotite, cordierite, sillimanite and feldspar) were calculated using the program Norm Version 4.0 (Ulmer, 1993) where $V^{VI}Fe^{+3} = V^{IV}Al^{+3} - (V^{VI}Al^{+3} + Cr_{TOTAL})$. The exceptions are for garnet where $Fe^{+3} = 2 - (Al^{VI} + Ti + Cr)$, and for sapphirine for which Fe^{+3} was calculated according to the methods of Higgins et al. (1979).

Garnet

Garnet in the sapphirine-bearing granulite samples (MM-208B and SS-077) is essentially a solid solution between almandine (44-54 mol%) and pyrope (48-54 mol%) while spessartine, grossular and andradite components sum up to 1.5 mol% (Table 1). Garnet composition does not vary significantly between samples or with grain size and chemical zonation is subtle (Figures 4 and 5). Grains involved

in reactions (1), (2) and (4) have compositions similar to cores of grains not involved in these reactions (Figure 5).

Orthopyroxene

Three different generations of orthopyroxene are present in the sapphirine-bearing granulite: (i) porphyroblasts (Opx_1) yielding Al_2O_3 contents between 10.40 and 10.69 wt.% (Table 2), which are usually unzoned, despite two analysed grains showing Al enrichment from core to rim (Figure 6); (ii) symplectites (Opx_2), together with sapphirine (Spr_2) and sillimanite (Sil_2), with Al_2O_3 contents varying between 8.46 and 10.07 wt.% (Table 2); and (iii) symplectites (Opx_3), together with cordierite, with Al_2O_3 contents varying between 6.92 and 7.7 wt% (Table 2). Other oxides do not show such large variations in any of the three generations (Table 2, Figure 6). X_{Mg} ratio ($Mg/Mg + Fe^{2+}$) for the first two generations is around 0.74-0.75 (Table 2), while in the third generation it is lower, from 0.70 to 0.75.

Table 1. Representative chemical composition of garnet of sapphirine-bearing granulite.

SAMPLES	MM-208-B	MM-208-B	MM-208-B	MM-208-B	SS-77	SS-77
ANALYSIS	49	50	87	91	13	15
REMARKS	Gt ₁ (Rim)	Gt ₁ (Core)	Gt ₁ (Rim)	Gt ₁ (Core)	Gt ₁ (Rim)	Gt ₁ (Core)
SiO ₂	39.60	39.43	39.93	39.85	39.69	39.76
TiO ₂	0.00	0.05	0.00	0.04	0.04	0.00
Al ₂ O ₃	22.73	22.84	23.24	23.35	22.66	22.32
Cr ₂ O ₃	0.01	0.07	0.00	0.08	0.06	0.02
FeO	22.51	23.07	22.24	23.24	23.95	24.24
MnO	0.57	0.44	0.40	0.29	0.36	0.33
MgO	13.58	13.55	13.87	14.26	12.76	12.93
CaO	0.43	0.43	0.58	0.51	0.50	0.54
Sum	99.43	99.88	100.26	101.62	100.02	100.14
Structural formula based on 12 oxygens						
Si	2.97	2.97	2.94	2.93	2.98	2.99
Al ^{IV}	0.02	0.02	0.06	0.07	0.01	0.01
Al ^{VI}	1.98	2.00	1.96	1.95	1.99	1.96
Ti	0.00	0.01	0.00	0.00	0.01	0.00
Cr	0.00	0.01	0.00	0.01	0.01	0.00
Fe ³⁺	0.04	0.01	0.10	0.12	0.02	0.05
Fe ²⁺	1.37	1.44	1.29	1.31	1.48	1.47
Mn	0.03	0.03	0.02	0.02	0.02	0.02
Mg	1.52	1.52	1.56	1.56	1.43	1.44
Ca	0.03	0.03	0.04	0.04	0.04	0.04
X _{Mg}	0.52	0.51	0.55	0.54	0.49	0.49
End-member molecular proportions (%)						
Alm	46.3	48.60	44.20	44.70	49.80	49.30
Pyr	51.30	51.20	53.50	53.30	48.00	48.50
Spe	1.20	0.10	0.80	0.60	0.80	0.70
Gro	1.20	0.10	1.50	1.40	0.10	1.50
And	0.00	0.00	0.03	0.02	0.00	0.01

Grt = Garnet.

Table 2. Representative chemical composition of orthopyroxene of sapphirine-bearing granulite.

SAMPLES	MM-208-B	MM-208-B	MM-208-B	MM-208-B	MM-208-B	MM-208-B	SS-77	SS-77	SS-77	
ANALYSIS	60	71	74	112	113	63	66	7	6	10
REMARKS	Opx ₁ (Core)	Opx ₁ (Core)	Opx ₁ (Core)	Opx ₂ (Core)	Opx ₂ (Core)	Opx ₃ (Core)	Opx ₃ (Core)	Opx ₂ (Core)	Opx ₃ (Core)	Opx ₃ (Core)
SiO ₂	48.66	48.25	48.25	48.58	48.43	50.08	51.46	49.08	50.00	49.79
TiO ₂	0.18	0.07	0.04	0.07	0.21	0.06	0.08	0.11	0.03	0.04
Al ₂ O ₃	10.69	10.40	10.61	10.07	9.88	6.92	7.44	8.46	7.53	7.73
Cr ₂ O ₃	0.04	0.08	0.02	0.02	0.06	0.07	0.05	0.00	0.00	0.09
FeO	15.95	17.07	16.93	16.37	16.37	17.38	15.45	18.49	19.23	19.13
MnO	0.21	0.21	0.06	0.12	0.09	0.11	0.17	0.26	0.22	0.00
MgO	24.15	24.10	23.77	24.23	24.35	25.01	25.07	22.99	23.33	22.80
CaO	0.06	0.01	0.00	0.03	0.00	0.00	0.00	0.00	0.03	0.01
Na ₂ O	0.02	0.00	0.00	0.01	0.02	0.00	0.00	0.00	0.00	0.03
Sum	99.96	100.19	99.68	99.50	99.41	99.73	99.72	99.39	100.37	99.64

Structural formula based on 6 oxygens										
Si	1.75	1.74	1.75	1.76	1.75	1.82	1.84	1.59	1.82	1.80
Al ^{IV}	0.25	0.26	0.25	0.24	0.24	0.18	0.16	0.32	0.18	0.19
Al ^{VI}	0.21	0.18	0.20	0.18	0.18	0.11	0.16	0.00	0.14	0.14
Ti	0.01	0.00	0.01	0.01	0.00	0.00	0.01	0.01	0.00	0.00
Cr	0.01	0.00	0.00	0.00	0.00	0.01	0.00	0.00	0.00	0.01
Fe ³⁺	0.03	0.07	0.05	0.06	0.06	0.06	0.00	0.13	0.04	0.05
Fe ²⁺	0.45	0.44	0.46	0.44	0.43	0.46	0.47	0.49	0.55	0.54
Mn	0.01	0.01	0.00	0.01	0.00	0.00	0.01	0.01	0.01	0.00
Mg	1.29	1.29	1.28	1.31	1.32	1.35	1.36	1.45	1.26	1.26
Ca	0.01	0.00	0.00	0.01	0.00	0.00	0.00	0.00	0.00	0.00
Na	0.01	0.00	0.00	0.00	0.00	0.00	0.00	0.00	0.00	0.01
XMg	0.74	0.74	0.74	0.75	0.75	0.75	0.74	0.75	0.70	0.70

Opx = Orthopyroxene.

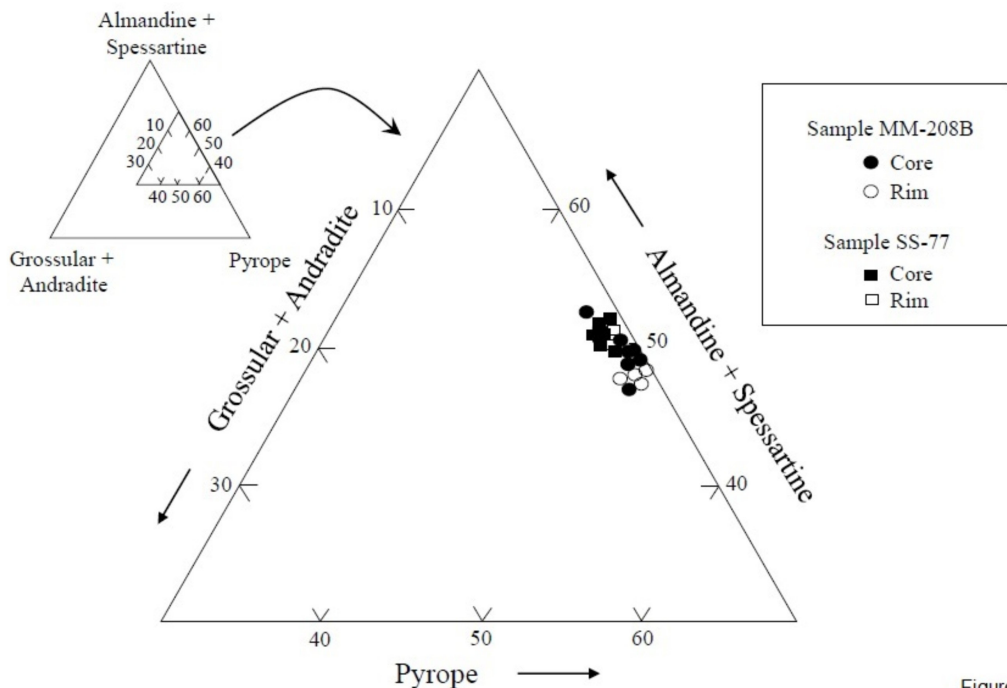


Figure 4

Figure 4. Pyrope – (grossular + andradite) – (almandine + spessartine) diagram for garnet (Grt1) from sapphirine-bearing granulite. While Fe + Mn, Ca and Mg are practically constant in the former, enrichment of Fe + Mn occurs in garnet (Grt₁) of the latter.

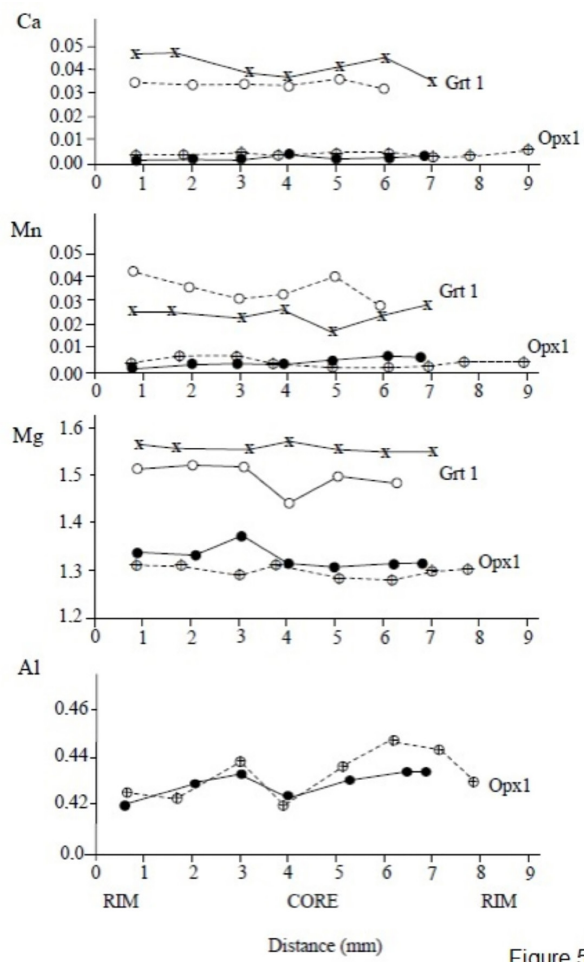


Figure 5

Figure 5. Microprobe profile through two porphyroblasts of garnet (Grt₁) and two porphyroblasts of orthopyroxene (Opx₁) (sample MM-208B) from UHT paragenesis of sapphirine-bearing granulite. For garnet, the vertical scale corresponds to the number of atoms per 12 O, and for orthopyroxene, number of atoms per 6 O.

Biotite

Biotite occurs in two forms: (i) Bt₁ formed at metamorphic peak conditions has polygonal contacts with Opx₁ (Figure 3A), and is mostly found in leucosome veins; and (ii) Bt₂ in symplectites with quartz around orthopyroxene grains, which are in contact with mesoperthite (Figure 3F). The compositions of (Bt₁) do not vary much, even from one sample to another (e.g. MM-208-B and SS-77), and are close to the phlogopite end member, with X_{Mg} from 0.78 to 0.86 (Table 3). Higher X_{Mg} (0.86) corresponds to lower TiO₂ contents (4.98 wt %), repeating the observations on biotite from other sapphirine-bearing granulites (e.g. Ouzegane and Boumaza, 1996; Guidotti, 1984; Henry and Guidotti, 2002). The second biotite type (Bt₂) is similar in chemical composition to the primary biotite (Bt₁), except for TiO₂ (4.98-5.23 wt % for Bt₁ and 3.12-4.16 wt % for Bt₂).

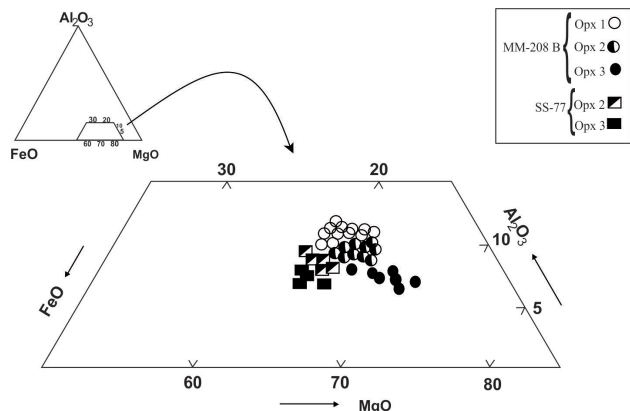


Figure 6. Compositional variations of coarse porphyroblast orthopyroxene (Opx₁) and symplectitic orthopyroxene (Opx₂ and Opx₃) in the Al₂O₃ - MgO - FeO (mol%) diagram. Note the decreasing of Al₂O₃ contents from (Opx₁) to (Opx₃) on the sapphirine-bearing granulite is noticeable.

Sapphirine

Sapphirine (Spr₁) included in Opx₁ and Grt₁ contains 63.39-64.66 wt.% Al₂O₃, which is somewhat higher than that of symplectitic sapphirine (Spr₂) (59.49 wt.% Al₂O₃) in symplectite intergrowth with (Opx₂) and (Sil₂) (Table 4). The chemical compositions of both types do not significantly depart from the theoretical ideal compositions with 7(Mg,Fe)O: 9(Al, Cr, Fe)₂O₃; 3 SiO₂, and 2(Mg, Fe)O: 2(Al, Cr, Fe)₂O₃; 1SiO₂ (Higgins et al., 1979) (Figure 7). No significant Tschermark coupled substitution [V^I(Mg, Fe)⁺² + IVSi⁺⁴ ⇌ V^I(Al, Fe)⁺³ + IVAl⁺³] occurred (Higgins et al., 1979; Higgins and Ribbe, 1979). Differences in contents for other oxides are minor, Na₂O and K₂O contents in both types being insignificant, and therefore not shown (Table 4).

Cordierite

Cordierite in sapphirine-bearing granulite samples MM-208-B and SS-77 is unzoned and displays the highest X_{Mg} of all ferromagnesian phases and shows X_{Mg} in the range of 0.70-0.88 (Table 5). Oxide totals are usually around 98%, suggesting the presence of minor amounts of H₂O or CO₂ as channel-filling molecular species in its structure (Carrington and Harley, 1996). The mineral is a product of reactions (3) and (4), and its formation is attributed to decompression, which occurred after the metamorphic peak conditions.

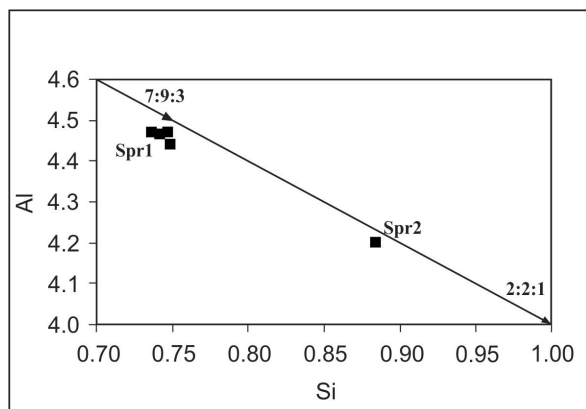
Sillimanite

The compositions of sillimanite Sil₁ in long prismatic crystals and Sil₂ in symplectites with Opx₂ are very similar. A representative composition of Sil₁ is given in Table 5. The high Fe content is a characteristic of sillimanite in UHT terrains, such as the Eastern Ghats Belt (Sengupta et al., 1990).

Table 3. Representative chemical composition of biotite of sapphirine-bearing granulite.

SAMPLES	MM-208-B	MM-208-B	SS-77	SS-77	SS-77
ANALYSIS	122	101	18	20	21
REMARKS	Bt ₁ (Core)	Bt ₂ (Core)	Bt ₁ (Core)	Bt ₂ (Rim)	Bt ₂ (Core)
SiO ₂	38.03	37.97	37.82	38.81	38.80
TiO ₂	5.23	4.16	4.98	3.64	3.12
Al ₂ O ₃	15.01	15.91	16.67	16.01	16.15
Cr ₂ O ₃	0.00	0.08	0.10	0.00	0.01
FeO	9.71	7.64	6.12	6.82	7.67
MnO	0.01	0.06	0.00	0.04	0.00
MgO	18.27	20.19	19.31	20.24	19.78
CaO	0.05	0.01	0.03	0.00	0.01
Na ₂ O	0.09	0.14	0.20	0.04	0.03
K ₂ O	9.98	9.97	9.52	10.28	9.88
H ₂ O	4.22	4.24	4.22	4.23	4.20
Sum	100.59	100.37	100.54	100.54	100.72
Structural formula based on 11 oxygens					
Si	2.72	2.68	2.69	2.75	2.77
Al ^{IV}	1.27	1.32	1.31	1.25	1.23
Al ^{VI}	0.01	0.00	0.08	0.09	0.13
Ti	0.27	0.22	0.26	0.19	0.17
Cr	0.01	0.01	0.01	0.00	0.00
Fe ³⁺	0.33	0.37	0.33	0.22	0.20
Fe ²⁺	0.18	0.03	0.00	0.16	0.23
Mn	0.01	0.01	0.00	0.01	0.00
Mg	1.94	2.13	2.05	2.14	2.10
Ca	0.01	0.01	0.01	0.00	0.01
Na	0.18	0.02	0.01	0.01	0.01
K	0.92	0.90	0.86	0.93	0.90
OH	2.00	2.00	2.00	2.00	2.00
XMg	0.78	0.84	0.86	0.85	0.83

Bt = Biotite.

**Figure 7.** Composition variation of sapphirine of sapphirine-bearing granulite in the Al-Si (a.p.f.u.) diagram. Spr=Sapphirine.

Feldspar

Plagioclase is essentially oligoclase ($An_{11-18}Ab_{81-88}$) with Na_2O contents between 9.29-9.53 wt.% in sample MM-208-B and 10.10-10.21 wt.% in sample SS-77 (Table 6).

K-feldspar in mesoperthite is orthoclase ($Ab_{8-15}Or_{85-92}$) in sample SS-77 (Table 6).

THERMOBAROMETRY, MICROSTRUCTURES RELATIONS AND P-T PATH

The sapphirine-bearing granulite paragenesis, $Grt_1 + Opx_1 + Sil_1 + Bt_1 + Spr_1$, is indicative of ultrahigh-temperature (UHT) metamorphism ($T > 900$ °C and $P = 7-11$ kbar; Harley, 1998). The high Al content in orthopyroxene (Opx_1), with $Al_2O_3 > 10$ wt.%, fits this inference. According to Hensen (1986) and Bertrand et al. (1991), the assemblage $Opx-Sil-Grt-Qtz$ should indicate pressures higher than 11 kbar. In order to constrain the temperature-pressure metamorphic conditions in the sapphirine-bearing granulite and the tonalitic orthogneiss, using the compositions of the cores of the grains, the thermobarometry programs by Kohn and Spear (1999), Reche and Martinez (1996), Berman (1991) and Holland and Powell (1998) were used (Table 7). The first two are EXCEL spreadsheets for thermobarometric

calculations applied to metapelites and based on calibrations by different authors. The last two (Berman, 1991; Holland and Powell, 1998) are based on multi-reaction calculations using consistent thermodynamic data.

The THERMOCALC software (Holland and Powell, 1998) made the calculation of all possible equilibria for the assemblage Pl-Opx-Sil-Grt-Bt-Kfs-Rt-Ilm-Qtz of the sapphirine-bearing granulite samples possible.

Table 4. Representative chemical composition of sapphirine of sapphirine-bearing granulite.

SAMPLES	MM-208-B	MM-208-B	MM-208-B	MM-208-B	MM-208-B
ANALYSIS	65	79	98	104	64
REMARKS	Spr ₁ (Core)	Spr ₂ (Core)	Spr ₁ (Core)	Spr ₁ (Core)	Spr ₁ (Core)
SiO ₂	12.49	14.77	12.60	11.59	12.38
TiO ₂	0.00	0.03	0.03	0.02	0.07
Al ₂ O ₃	63.82	59.49	63.39	64.66	63.80
Cr ₂ O ₃	0.09	0.14	0.19	0.07	0.09
FeO	7.16	6.75	6.52	6.91	7.28
MnO	0.04	0.08	0.02	0.07	0.10
MgO	16.41	17.60	16.94	16.58	16.30
Sum	100.01	98.86	99.90	99.94	100.18
Structural formula based on 10 oxygens					
Si	0.74	0.88	0.75	0.69	0.73
Al	4.46	4.20	4.44	4.53	4.47
Ti	0.00	0.00	0.00	0.00	0.00
Cr	0.01	0.06	0.01	0.01	0.04
Fe (Total)	0.35	0.34	0.32	0.34	0.36
Mn	0.00	0.00	0.00	0.00	0.00
Mg	1.45	1.57	1.50	1.47	1.44
XMg	0.80	0.82	0.82	0.81	0.80

Spr = Sapphitine.

Table 5. Representative chemical composition of cordierite and sillimanite of sapphirine-bearing granulite.

SAMPLES	MM-208-B	MM-208-B	SS-77	SS-77	MM-208-B
ANALYSIS	12	13	9	19	97
REMARKS	Crd (Core)	Crd (Core)	Crd (Core)	Crd (Core)	Sil1 (Core)
SiO ₂	48.56	48.97	49.83	49.81	36.49
TiO ₂	0.04	0.00	0.00	0.00	0.00
Al ₂ O ₃	32.84	33.15	33.30	33.42	63.52
Cr ₂ O ₃	0.05	0.05	0.00	0.12	0.03
FeO	5.50	4.91	4.30	4.02	1.27
MnO	0.11	0.10	0.00	0.01	0.13
MgO	10.34	10.90	10.65	10.76	0.00
CaO	0.02	0.00	0.01	0.00	0.01
Na ₂ O	0.03	0.03	0.06	0.06	0.02
K ₂ O	0.01	0.00	0.00	0.03	0.03
Sum	97.50	98.11	98.15	98.77	101.50
Structural formula based on 18 oxygens					
Si	4.98	4.97	5.03	5.03	1.95
Al (Total)	3.97	3.97	3.96	3.94	4.01
Ti	0.03	0.00	0.00	0.00	0.00
Cr	0.01	0.01	0.00	0.01	0.00
Fe (Total)	0.47	0.42	0.36	0.34	0.06
Mn	0.01	0.01	0.00	0.00	0.01
Mg	1.58	1.65	1.60	1.65	0.00
Ca	0.00	0.00	0.00	0.00	0.00
XMg	0.88	0.70	0.72	0.73	0.00

Crd = Cordierite; Sil = Sillimanite.

Table 6. Representative chemical composition of feldspars of sapphirine-bearing granulite.

SAMPLES	MM-208-B	MM-208-B	MM-208-B	SS-77	SS-77	SS-77	SS-77
ANALYSIS	67	68	102	26	29	28	30
REMARKS	Pl ₁ (Core)	Mp ₁ (Core)	Mp ₁ (Core)				
SiO ₂	63.90	64.28	64.05	64.41	65.75	64.41	64.41
TiO ₂	0.00	0.00	0.00	0.03	0.03	0.02	0.01
Al ₂ O ₃	22.86	22.75	22.41	22.17	21.81	18.50	18.61
Cr ₂ O ₃	0.03	0.02	0.02	0.20	0.34	0.00	0.00
FeO	0.33	0.21	0.17	0.00	0.00	0.22	0.21
MnO	0.06	0.00	0.04	0.16	0.00	0.00	0.00
CaO	3.67	3.50	3.72	3.01	2.30	0.04	0.02
Na ₂ O	9.29	9.52	9.53	10.21	10.10	0.89	0.89
K ₂ O	0.26	0.20	0.45	0.14	0.06	15.50	15.66
Sum	100.40	100.48	100.39	100.55	100.69	99.58	99.81
Structural formula based on 8 oxygens							
Si	2.81	2.82	2.82	2.84	2.88	2.98	2.97
Al ^{IV}	1.19	1.18	1.16	1.15	1.13	1.02	1.01
Ti	0.00	0.00	0.00	0.00	0.00	0.00	0.00
Cr	0.00	0.00	0.00	0.01	0.01	0.01	0.00
Fe ³⁺	0.01	0.01	0.01	0.01	0.00	0.00	0.00
Fe ²⁺	0.00	0.00	0.00	0.00	0.00	0.01	0.00
Mn	0.00	0.00	0.00	0.00	0.00	0.00	0.00
Ca	0.17	0.16	0.17	0.14	0.11	0.00	0.00
Na	0.79	0.81	0.81	0.87	0.86	0.15	0.08
K	0.02	0.01	0.02	0.01	0.01	0.83	0.92
End-member proportions (mol%)							
An	18	17	17	14	11	-	-
Ab	81	82	81	85	88	15	8
Or	1	1	2	1	1	85	92

Pl = Plagioclase; Mp = Mesopertite.

Table 7. Geothermobarometric data from study rocks.

SAMPLES	SOFTWARES/ METHODS	Kohn and Spear (1999)	Reche and Martinez (1996)	TWEEQU Berman (1991) Grt-Bt	THERMOCALC Holland and Powell (1998) (Pl-Opx-Sil-Grt-Bt-Fk-Rt-Ilm-Qtz)
MM - 208B	Thermometer				
	Grt - Opx	770-810°C	710-800°C	730-750°C	
	Grt - Bt	-	500-600°C	580-720°C	
	Bt - Opx	-	920-1020°C	890-1010°C	
	Barometer				
	PI - Grt - Sil - Qtz	6-7.5 kbar	10-12 kbar	-	
SS-77	PI - Grt - Sil - Qtz	7.5 kbar	-	6.0-7.5 kbar	900 - 1000°C 8.4 - 11.1 kbar
	Thermometer				
	Grt - Opx	780-820°C	670-800°C	730-780°C	
	Grt - Bt	-	510-660°C	580-650°C	
	Bt - Opx	-	940-1010°C	880-1000°C	
SS-77	Barometer				
	PI - Grt - Sil - Qtz	6.5-7.5 kbar	11-13 kbar	-	
	Opx - Grt - PI - Qtz	7.5-9.5 kbar	-	8.0-9.0 kbar	

Grt = Garnet; Opx = Orthopyroxene; Bt = Biotite; Sil = Sillimanite; Qtz = Quartz; Pl = Plagioclase; Fk = KFeldspar; Rt = Rutile; Ilm = Ilmenite.

The estimated pressure and temperature data calculated with THERMOCALC (8.4-11.1 kbar and 900-1000 °C, Table 7) retrieve the metamorphic peak at ultrahigh-temperature conditions. For the temperature interval of 900-1000 °C, the different calibrations of the geobarometer Opx-Grt-Pl-Qz

(Bhattacharya et al., 1991) lead to pressure that are compatible with those obtained by THERMOCALC. The geobarometer Pl-Grt-Sil-Qtz (Kohn and Spear, 1999; Reche and Martinez, 1996) gave widely different results (6-12 kbar) (Table 7). Common geothermometers, based on Fe-Mg exchange

reactions, such as Grt-Opx (Sen and Bhattacharya, 1984; Harley, 1984; Lee and Ganguly, 1988; Kohn and Spear, 1999; Reche and Martinez, 1996; Berman, 1991) and Grt-Bt (Thompson, 1976; Holdaway and Lee, 1977; Perchuk and Lavrent'eva, 1983; Reche and Martinez, 1996; Berman, 1991), yield lower temperature ranges, 710-810 °C for the first pair and 500-720 °C for the second. Such values are incompatible with ultrahigh-temperature conditions, as revealed by the primary paragenesis, and might reflect continuous Fe-Mg exchange between mineral pairs during retrograde metamorphism. The same Fe-Mg re-equilibrium is expected for the pair Bt-Opx (Sengupta et al., 1990), but this geothermometer indicates very high temperatures. Except for those obtained with THERMOCALC (Holland and Powell, 1998), we interpret these results as misleading because X_{Mg} ratios for the two minerals chosen for calculations are very close (Tables 2 and 3), probably increasing the error.

In the sapphirine-bearing granulite, the near-peak paragenesis is garnet-orthopyroxene-sillimanite-quartz or sapphirine-orthopyroxene±mesoperthite-plagioclase-rutile-ilmenite-magnetite. There is no petrographic evidence for the presence of the association Spr + Qtz. The reactions $\text{Grt}_1 + \text{Opx}_1 = \text{Opx}_2 + \text{Spr}_2 (\pm \text{Sil})$ (reaction 2), $\text{Opx}_1 + \text{Sil}_1 + \text{Qtz} = \text{Crd}$ (reaction 3) and $\text{Grt}_1 + \text{Qtz} = \text{Opx}_3 + \text{Crd}$ (reaction 4) that formed symplectitic coronas around the garnet and orthopyroxene porphyroblasts represent a retrograde evolution. Reactions (3) and (4) define low slope curves and represent decompression paths. Nevertheless, it is more probable that they were related to a temperature drop since the Al content of Opx_3 is always lower than that for Opx_1 . On the other hand, the symplectites of $\text{Bt}_2 + \text{Qz}$ formed by reaction $\text{Opx}_{1-2} + \text{Mp} + \text{H}_2\text{O} = \text{Bt}_2 + \text{Qtz}$ (reaction 5) are also retrograde, related to temperature decrease even in the presence of water (Figure 8).

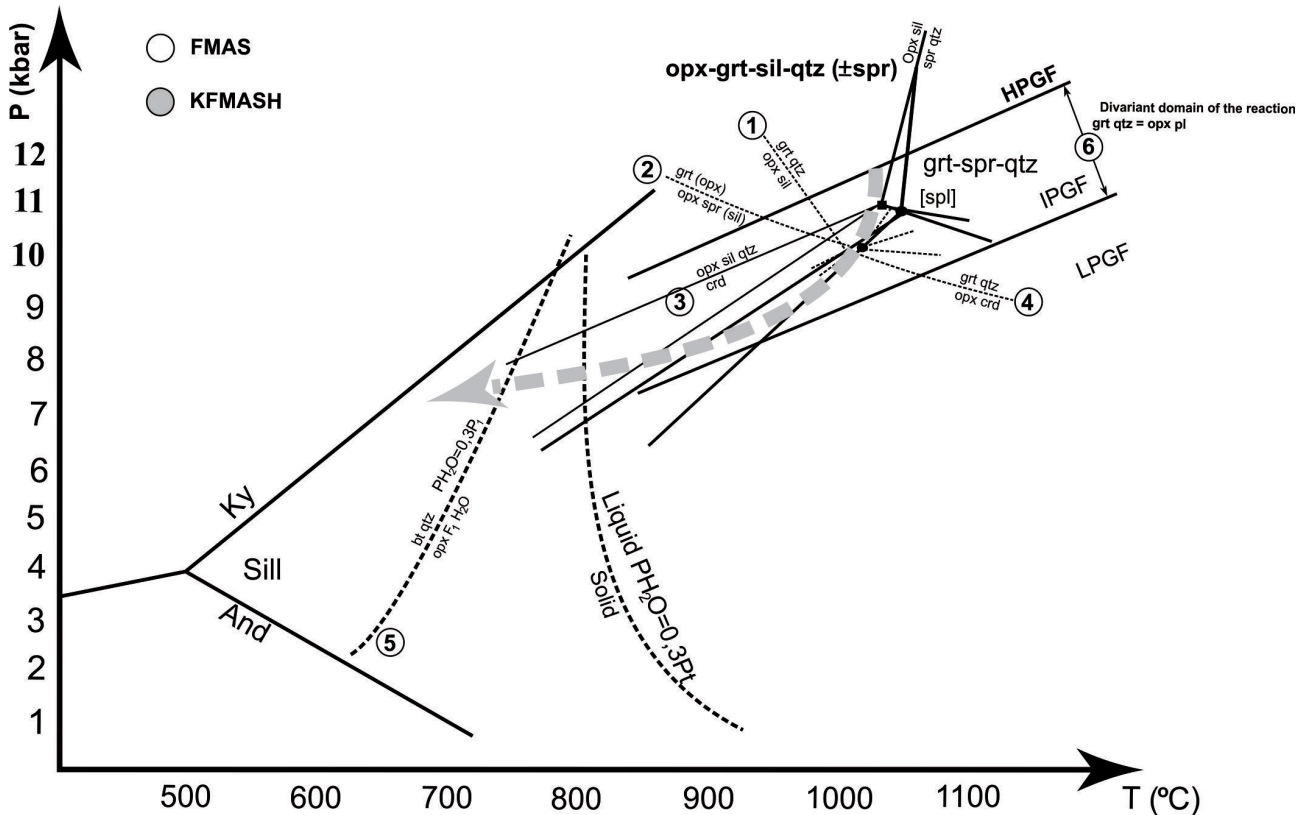


Figure 8. P-T diagram with the P-T path inferred from the sapphirine-bearing granulite: spinel absent invariant point and univariant reactions in the FMAS system involving garnet, orthopyroxene, sapphirine, cordierite, spinel, sillimanite and quartz. The field of the assemblages grt-spr-qtz and opx-grt-sill-qtz is also shown. The divariant reaction (6) limits the high-pressure domain (HPGF), intermediate pressure (IPGF) and low-pressure granulite (LPGF) facies respectively (Green and Ringwood, 1972). The granite-melt curve in the KFMASH system is after Vielzeuf and Holloway (1988). The alumino-silicate triple point is after Holdaway and Mukhopadhyay (1995). Reaction (1) is after Sengupta et al. (1990); reaction (2) after Harley and Hensen (1990); reaction (3) after Harris and Holland (1984); reaction (4) after Waters (1991); reaction (5) after Harley (1989); reaction (6) after Green and Ringwood (1972). The circles and squares symbols shown in the reactions were extracted from the authors already mentioned in the legend. The reactions are described in detail in the text. Abbreviations follow Kretz (1983) and Whitney and Evans (2010).

DISCUSSION AND CONCLUSIONS

Sapphirine-bearing granulite of the ISCB segment records UHT metamorphic conditions. The metamorphic peak reached conditions of 900-1000 °C at 8.4-11.1 kbar. The Al_2O_3 contents (>10 wt.%) and TiO_2 (>5 wt.%) in the orthopyroxene and biotite porphyroblast cores attest to the UHT peak conditions (Leite et al., 2009). Sapphirine-bearing granulites are found as small relics in high-grade metamorphic belts. They are important since their mineral parageneses record anomalously high temperatures compared to their host granulites.

In the geodynamic context, the origin of granulite terranes has been related to collision tectonics (Raith et al., 1997), although authors such as England and Thompson (1986) believe that crustal thickening alone is incapable of generating the temperatures necessary for granulite facies metamorphism. The P-T path derived in this study (Figure 8) is compatible with a retrograde portion of a clockwise P-T path that occurred accompanying crustal thickening during an orogenic cycle (e.g. Bohlen, 1987; Harley, 1989). The thrusting of the Itabuna Belt over the Jequié Block (Barbosa and Sabaté, 2002, 2004) was part of a collisional event, and the associated metamorphism that took place in the region close to 2081 ± 20 Ma (Silva et al., 2002; Pinho, 2005; Leite et al., 2009) reached UHT conditions, leading to the crystallization of the sapphirine-bearing granulite.

What was the heat source that raised the temperature high enough to cause partial melting of these rocks? The addition of radioactive material (Harley, 1989) might have caused heating during the overthrusting mentioned above, but intuitively it is thought that this would have been insufficient to cause such a large temperature rise. Underplating or intrusion of mantle-derived basaltic magmas (Ellis, 1980; Bohlen, 1991) could have been the heat source, and the differentiation of these magmas could have produced the tonalite protoliths for the regional orthogneisses (Pinho, 2005).

The ages of the protoliths are around 2.15-2.13 Ga, obtained by U-Pb SHRIMP, Pb-Pb evaporation on zircon, and Pb-Pb whole rock isochrons (Corrêa-Gomes, 2000; Corrêa-Gomes and Oliveira, 2002; Silva et al., 2002; Pinho, 2005), while the age of the metamorphism is close to 2.0 Ga (Barbosa and Sabaté, 2004), determined by the U-Th-Pb microprobe method on monazite (Montel et al., 1994, 1996), or around 2.07-2.08 Ga, found for overgrowths on plutonic zircon by the U-Pb SHRIMP method (Silva et al., 2002; Pinho, 2005).

Hence, accretion of radioactive material together with the presence of basaltic magma in the ISBC roots could have produced the high temperatures necessary for the formation of the sapphirine-bearing granulites, and also the partial melting that generated the associated leucosome veins. The protoliths of the sapphirine-bearing granulites could have been metapelites (Ouzegane and Boumaza, 1996; Moraes et al., 2002), which, subjected to extreme temperatures,

would have partially melted, leaving the sapphirine-bearing granulite as the refractory residue. A significant quantity of melt must have drained away, although sufficient remained behind in the form of leucosome veins, which must have formed at the metamorphic peak after the ductile deformation (F1, F2, F3) (Barbosa, 1986, 1990; Seixas, 1993). Polygonal biotite (Bt_1) may have crystallized from melt involved in the reactions. Biotite (Bt_2) with lower Ti content in symplectites with quartz was formed during retrograde metamorphism during regional cooling.

The common granulite host rocks, including the tonalitic orthogneiss, may also have experienced UHT metamorphism conditions, but any record of this was probably obliterated during the extensive retrograde event that affected the area, similarly to the Brasília Fold Belt evolution (Moraes et al., 2002). The retrograde path can be defined using the reactions that were probably responsible for the destruction of UHT minerals, and shown in Figure 8.

ACKNOWLEDGEMENTS

We acknowledge the fellowship from Project 381/02 – CAPES-COFECUB, the support from CBPM – Companhia Baiana de Pesquisa Mineral, and the revision of the English manuscript by Professors E. Sampaio and Ian McReath. The authors thank the anonymous reviewer for comments on this paper.

REFERENCES

- Aillon, M. P. (1992). *Caracterização petroquímica e do metamorfismo das rochas granulíticas da região de Cachoeira-São Felix-Cruz das Almas, Bahia*. Dissertação (Mestrado). Salvador: Universidade Federal da Bahia.
- Alibert, C., Barbosa, J. S. F. (1992). Ages U-Pb déterminés à la "SHRIMP" sur des zircons du Complexe de Jequié, Craton du São Francisco, Bahia, Brésil. *14 Réunion Science de la Terre*, p. 4. Toulouse: Societe Geologique de France.
- Alkmim, F. F., Brito Neves, B. B., Alves, J. A. C. (1993). Arcabouço tectônico do Cráton do São Francisco: uma revisão. In: J. M. L. Dominguez, A. Misi (Eds.), *O Cráton do São Francisco*, v. 1, 45-62. Salvador: SBG.
- Almeida, F. F. M. (1977). O Cráton do São Francisco. *Revista Brasileira de Geociencias*, 7, 349-364.
- Almeida, F. F. M., Hasui, Y., Brito Neves, B. B. (1976). The Upper Precambrian of South America. *Boletim IG, USP*, 7, 45-80.
- Alves da Silva, F. C., Barbosa, J. S. F., Damasceno, J. A., Rodrigues, Z. R. C., Paim, M. (1996). Estrutura Dômica

- de Brejões (SE-Bahia): padrão de interferência, produto de anomalia termal ou feição ignea preservada? *XXXIX Congresso Brasileiro de Geologia, Salvador (BA)*, v. 6, 266-269.
- Arima, M., Grower, C. F. (1991). Osumulite-bearing granulites in the eastern Greenville province, eastern Labrador, Canada. *Journal of Petrology*, 32, 29-61.
- Baldwin, J., Powell, R., Brown, M., Moraes, R., Fuck, R. A. (2005). Modelling of mineral equilibria in ultrahigh-temperature metamorphic rocks from the Anápolis-Itaú Complex, central Brazil. *Journal of Metamorphic Geology*, 23(7), 511-531.
- Barbosa, J. S. F. (1986). *Constitution lithologique et métamorphique de la région granulitique du sud de Bahia, Brésil*. Thèse (Doctorat). Paris: Université Pierre et Marie Curie.
- Barbosa, J. S. F. (1990). The granulites of the Jequié Complex and Atlantic Mobile Belt, Southern Bahia, Brazil: an expression of Archean Proterozoic Plate Convergence. In: D. Vielzeuf, P. H. Vidal (Eds.), *Granulites and crustal evolution*, 195-221. Springer-Verlag: Clermont Ferrand.
- Barbosa, J. S. F. (1996). O embasamento arqueano e proterozoico inferior do Estado da Bahia. In: Eds) J. S. F. Barbosa, J. M. L. Dominguez (Eds.), *Geologia da bahia: texto explicativo para o Mapa Geológico ao Milionésimo*, 63-84. (SICM/SGM, Publicação Especial).
- Barbosa, J. S. F., Dominguez, J. M. L. (1996). *Texto explicativo para o Mapa Geológico ao Milionésimo*, 400 p. (SICM/SGM, Publicação Especial).
- Barbosa, J. S. F., Fonteilles, M. (1989). Caracterização dos protólitos da região granulítica do sul da Bahia. *Revista Brasileira de Geociencias*, 19(1), 3-16.
- Barbosa, J. S. F., Fonteilles, M. (1991). Síntese sobre o metamorfismo da região granulítica do sul da Bahia, Brasil. *Revista Brasileira de Geociencias*, 21(4), 328-341.
- Barbosa, J. S. F., Sabaté, P. (2002). Geological features and the Paleoproterozoic collision of four Archean crustal segments of the São Francisco Craton, Bahia, Brazil. A synthesis. *Anais da Academia Brasileira de Ciencias*, 74(2), 343-359.
- Barbosa, J. S. F., Sabaté, P. (2004). Archean and Paleoproterozoic crust of the São Francisco Craton, Bahia, Brazil: geodynamic features. *Precambrian Research*, 133, 1-27.
- Barbosa, J. S. F., Cruz, S. P. C., Souza-Oliveira, J. S. (2012). Terrenos Metamórficos do Embasamento. In: J. S. F. Barbosa, J. F. Mascarenhas, L. C. Correa-Gomes, J. M. L. Dominguez, J. S. de Oliveira., *Geologia da Bahia: pesquisa e atualização*, 101-199.
- Bastos Leal, L. R. (1998). *Geocronologia U/Pb (SHRIMP) 207Pb/206Pb, Rb/Sr, Sm/Nd e K/Ar dos terrenos Granito-Greenstone do Bloco Gavião: Implicações para a evolução Arqueana e Proterozóica do Cráton do São Francisco, Brazil*. Tese (Doutorado). São Paulo: Instituto de Geociências – USP.
- Berman, R. G. (1991). TWEEQU: thermobarometry using multi-equilibrium calculations: a new technique with petrological applications. *Canadian Mineralogist*, 29, 833-855.
- Bertrand, P., Ellis, D. J., Green, H. (1991). The stability of sapphirine-quartz and hypersthene-sillimanite-quartz assemblages: an experimental investigation in the system FeO-MgO-Al₂O₃-SiO₂ under H₂O and CO₂ conditions. *Contributions to Mineralogy and Petrology*, 108, 55-71.
- Bhattacharya, A., Krishnakumar, K. R., Raith, M., Sen, S. K. (1991). An improved set of a-X parameters of Fe-Mg-Ca garnets and refinements of the orthopyroxene-garnet thermometer and orthopyroxene-garnet-plagioclase-garnet barometer. *Journal of Petrology*, 32, 629-665.
- Bohlen, S. R. (1987). Pressure-temperature-time paths and a tectonic model for evolution of granulites. *The Journal of Geology*, 95, 617-632.
- Bohlen, S. R. (1991). On the formation on granulites. *Journal of Metamorphic Geology*, 9, 223-229.
- Caby, R., Bertrand, J. M., Blac, R. (1981). Pan-African ocean closure and continental collision in the Hoggar-Iforas segment, central Sahara. In: A. Kröner (Ed.), *Developments in Precambrian Geology 4: Precambrian plate tectonics*, 407-434. Elsevier.
- Carrington, D. P., Harley, S. L. (1996). Cordierite as a monitor of fluid and melt H₂O contents in the lower crust: an experimental calibration. *Geology*, 24, 647-650.
- Cordani, U. G. (1973). *Evolução Geológica Precambriana da Faixa Costeira do Brasil entre Salvador e Vitória*. Tese (Livre Docência). São Paulo: Instituto de Geociências – USP.
- Cordani, U. G., Iyer, S. S., Taylor, P. N., Kawashita, K., Sato, K., McCreath, I. (1992). Pb/Pb, Rb/Sr, and K-Ar sistematic of the Lagoa Real uranium province (south-central Bahia, Brazil) and the Espinhaço Cycle (ca. 1.5-1.0 Ga). *Journal of South American Earth Sciences*, 5(1), 33-36.
- Corrêa-Gomes, L. C. (2000). *Evolução dinâmica da zona de cisalhamento neoproterozóica de Itabuna-Itaju do Colonia e do magmatismo fissural alcalino associado (SSE do Estado da Bahia, Brasil)*. Tese (Doutorado). Campinas: UNICAMP.
- Corrêa-Gomes, L. C., Oliveira, E. P. (2002). Dados Sm/Nd, Ar/Ar e Pb/Pb de corpos plutônicos do Sudeste da Bahia, Brasil: implicações para o entendimento para a evolução tectônica no limite Orógeno Araçuaí/Cráton do São Francisco. *Revista Brasileira de Geociencias*, 32(2), 185-196.

- Cunha, J. C., Fróes, R. J. B. (1994). *Komatiítos com textura "spinifex" do Greenstone Belt de Umburanas*, 29 p. Salvador: CBPM. (Special Publication).
- Cunha, J. C., Bastos Leal, L. R., Fróes, R. J. B., Teixeira, W., Macambira, M. J. B. (1996). Idade dos Greenstone Belts e dos terrenos TTGs associados da Região do Cráton do São Francisco (Bahia, Brasil). *XXIX Congresso Brasileiro de Geologia*, v. 1, 62-65. Salvador: SBG-BA.
- Cunha, J. C., Barbosa, J. S. F., Mascarenhas, J. F. (2012). Greenstone Belts e Sequencias Similares. In: J. S. F. Barbosa, J. F. Mascarenhas, L. C. Correa-Gomes, J. M. L. Dominguez, J. S. de Oliveira. *Geologia da Bahia: pesquisa e atualização*, 203-325. CBPM-UFBA. (Edição Especial).
- Dallwitz, W. B. (1986). Co-existing sapphirine and quartz in granulite from Enderby Land, Antarctica. *Nature*, 219, 476-477.
- Dasgupta, S., Sengupta, P., Ehl, J., Raith, M., Bardhan, S. (1995). Reaction textures in a suite of spinel granulites from Eastern Ghats Belt, India: evidence for polymetamorphism, a partial petrogenetic grid in the system KFMASH and the role of ZnO and Fe₂O₃. *Journal of Petrology*, 36, 435-461.
- Ellis, D. J. (1980). Osumulite-sapphirine and quartz in granulite from Enderby Land, Antarctica: P-T conditions of metamorphism, implications for garnet-cordierite equilibria and the evolution of deep crust. *Contributions to Mineralogy and Petrology*, 74, 201-210.
- England, P. C., Thompson, A. B. (1986). Some thermal and tectonic models for crustal melting in continental collision zones. In: Coward, M.P. e Ries, A.C. (eds) *Collision Tectonics. Special Publication*, 19, 83-94. London: Geology Society.
- Figueiredo, M. C. H. (1989). Geochemical Evolution of Eastern Bahia, Brazil: A probably early-Proterozoic subduction-related magmatic arc. *Journal of South American Earth Sciences*, 2(2), 131-145.
- Figueiredo, M. C. H., Barbosa, J. S. F. (1993). Terrenos Metamórficos de Alto Grau do Cratôn do São Francisco. In: J. M. L. Dominguez, A. Missi (Eds.), *O Cratôn do São Francisco*, 63-83. SBG/SGM/CNPq. (Publicação Especial).
- Fornari, A. (1992). *Petrologia, geoquímica e metamorfismo das rochas enderbíticas-charnockíticas da região de Lage e Mutuipe, Bahia*. Dissertação (Mestrado). Salvador: Universidade Federal da Bahia.
- Gonçalves, P., Nicollet, C., Montel, J. M. (2004). Petrology and in-situ U-Th-Pb monazite geochronology of Ultra-High Temperature metamorphism from the Andriamena mafic unit, north-central Madagascar: significance of a petrographical PT path in a polymetamorphic context. *Journal of Petrology*, 45(10), 1923-1957.
- Green, D. H., Ringwood, A. E. (1972). A comparaison of recent experimental data on the gabbro - garnet granulite - eclogite transition. *The Journal of Geology*, 80, 277-288.
- Grew, E. S. (1980). Sapphirine+quartz association from Archean rocks of Enderby Land, Antarctica. *The American Mineralogist*, 65, 821-836.
- Grew, E. S. (1982). Sapphirine, kornerupine and sillimanite-orthopyroxene in the charnockitic region of south India. *Journal of the Geological Society of India*, 23, 469-505.
- Guidotti, C. V. (1984). Micas in metamorphic rocks. In: S. W. Bayley (Ed.), *Micas: Mineralogical Society of America Reviews in Mineralogy*, 13, 357-468.
- Harley, S. L. (1984). An experimental study of the partitioning of Fe and Mg between garnet and orthopyroxene. *Contributions to Mineralogy and Petrology*, 36, 359-373.
- Harley, S. L. (1989). The origin of granulites: a metamorphic perspective. *Geological Magazine*, 126, 215-247.
- Harley, S. L. (1998). On the occurrence and characterization of ultrahigh-temperature crustal metamorphism. In: P. J. Treloar, P. J. O'Brien (Eds.), *What drives metamorphism and metamorphic reactions?*, 138, 81-107. London: Geological Society. (Special Publications).
- Harley, S. L., Hensen, B. J. (1990). Archaean and Proterozoic high-grade terranes of East Antarctica (40-80° E): a case study of diversity in granulite facies metamorphism. In: J. R. Ashworth, M. Brown (Eds.), *High-temperature metamorphism and crustal anatexis*, 320-370. London: Unwin Hyman.
- Harris, N. B. W., Holland, T. J. B. (1984). The significance of cordierite-hypersthene assemblages from the Bertioga-region of the Central Limpopo belt: evidence for rapid decompression in the Archean? *The American Mineralogist*, 69, 1036-1049.
- Henry, D. J., Guidotti, C. V. (2002). Ti in biotite from metapelitic rocks: temperature effects, crystallochemical controls and petrologic applications. *The American Mineralogist*, 87, 375-382.
- Hensen, B. J. (1986). Theoretical phase relations involving cordierite and garnet revisited the influence of oxygen fugacity on the stability of sapphirine and spinel in the system Mg-Fe-Al-Si-O. *Contributions to Mineralogy and Petrology*, 92, 362-367.
- Higgins, J. B., Ribbe, P. H. (1979). Sapphirine II. A neutron and X-Ray diffraction study of (Mg-Al)VI(Si-Al)IV ordering in monoclinic sapphirine. *Contributions to Mineralogy and Petrology*, 68, 357-368.
- Holdaway, M. J., Lee, S. M. (1977). Fe-Mg cordierite stability in high-grade pelitic rocks based on experimental, theoretical

- and natural observations. *Contributions to Mineralogy and Petrology*, 63, 175-198.
- Higgins, J. B., Ribbe, P. H., Herd, R. K. (1979). Sapphirine I. Crystal chemical contributions. *Contributions to Mineralogy and Petrology*, 68, 349-356.
- Holdaway, M. J., Mukhopadhyay, J. (1995). Thermodinamics properties of stoichiometric staurolite $H_2Fe_4Al_18Si_8O_{48}$ and $H_6Fe_2Al_18Si_8O_{48}$. *The American Mineralogist*, 80, 520-533.
- Holland, T., Powell, R. (1998). An internally consistent thermodynamic data set for phases of petrological interest. *Journal of Metamorphic Geology*, 16, 309-343.
- Iwamura, S., Tsunogae, T., Kato, M., Koizumi, T., Dunkley, D. J. (2013). Petrology and phase equilibrium modelling of spinel-sapphirine-bearing mafic granulite from Akarui Point, Lützow-Holm Complex, East Antarctica: implications for the P-T path. *Journal of Mineralogical and Petrological Sciences*, 108, 345-350.
- Iyer, S. S., Barbosa, J. S. F., Choudhuri, A., Krouse, H. S. (1995). Possibles sources de CO₂ in granulite facies rocks: carbon isotope evidence from the Jequié Complex, Brazil. *Petrology*, 3, 226-237.
- Kelsey, D. E., Hand, M. (2015). On ultrahigh temperature crustal metamorphism: phase equilibria, trace element thermometry, bulk composition, heat sources, timescales and tectonic settings. *Geoscience Frontiers*, 6, 311-356.
- Kienast, J. R., Ouzegane, K. (1987). Polymetamorphic Al-Mg rich parageneses in Archean rocks from Hoggar, Algeria. *Geological Journal*, 22, 57-79.
- Kohn, M. J., Spear, F. S. (1999). Program thermobarometry. Acessado em 01 de maio de 2015, <[http://ees2.geo.rpi.edu/MetaPetaRen/Software/GTB_Prog/GTB\(Feb%2021,2001\)/GTB_2.0_manual.pdf](http://ees2.geo.rpi.edu/MetaPetaRen/Software/GTB_Prog/GTB(Feb%2021,2001)/GTB_2.0_manual.pdf)>.
- Kretz, R. (1983). Symbols for rock-forming minerals. *The American Mineralogist*, 68, 277-279.
- Kriegsman, L. M. (1996). Divariant and trivariant reaction line slopes in FMAS and CFMAS: theory and applications. *Contributions to Mineralogy and Petrology*, 126(1), 38-50.
- Ledru, P., Cocherie, A., Barbosa, J. S. F., Johan, V., Onstott, T. (1994). Âge du métamorphisme granulitique dans le Craton du São Francisco (Brésil). Implications sur la nature de l'orogène transamazonien. *C.R. Académie des Sciences de Paris*, 211, 120-125.
- Lee, H. Y., Ganguly, J. (1988). Equilibrium compositions of coexisting garnet and orthopyroxene: experimental determinations in the system FeO-MgO-Al₂O₃-SiO₂ and applications. *Journal of Petrology*, 29, 93-113.
- Leite, C. M. M. (2002). *A evolução Geodinâmica da Orogênese Paleoproterózoica nas Regiões de Capim Grosso - Jacobina e Pintadas - Mundo Novo (Bahia, Brasil): metamorfismo, anatexia crustal e tectônica*. Tese (Doutorado). Salvador: Instituto de Geociências – UFBA.
- Leite, C. M. M., Barbosa, J. S. F., Goncalves, P., Nicollet, C., Sabaté, P. (2009). Petrological evolution of silica-undersaturated sapphirine-bearing granulite in the Paleoproterozoic Salvador-Curaçá Belt, Bahia, Brazil. *Gondwana Research*, 15, 49-70.
- Marinho, M. M. (1991). *La séquence volcano-sédimentaire de Contendas-Mirante et la bordure occidentale du bloc Jequié (Craton du São Francisco-Brésil): un exemple de transition Archean-Protérozoïque*. Thèse (Doctorat). Clermont Ferrand: Université Blaise Pascal.
- Marinho, M. M., Vidal, Ph., Alibert, C., Barbosa, J. S. F., Sabaté, P. (1992). Geochronology of the Jequié-Itabuna granulitic belt and the Contendas-Mirante Volcano-Sedimentary belt. In: A. Kröner, S. Moorbath (Eds.), *Petrologic and Geochronologic evolution of the oldest segments of the São Francisco Craton, Brazil*. Boletim IG-USP. Série Científica, 17, 73-96.
- Martin, H., Sabaté, P., Peucat, J. J., Cunha, J. C. (1991). Un segment de croûte continentale d'âge archéen ancien (3,4 milliards d'années): le Massif de Sete Voltas (Bahia-Brésil). *Comptes Rendus de l'Academie des Sciences de Paris*, 313, série II, 531-538.
- Mascarenhas, J. F., Silva, E. F. A. (1994). Greenstone Belt de Mundo Novo (Bahia): caracterização e implicações metalogenéticas no Craton do São Francisco. *CBPM, Special Publication, Brazil*, 32 p.
- Menezes Leal, A. B., Santos, A. L. D., Bastos Leal, L. R., Cunha, J. C. (2015). Geochemistry of contaminated komatiites from the Umburanas greenstone belt, Bahia State, Brazil. *Journal of South American Earth Sciences*, 61, 1-13.
- Montel, J. M., Foret, S., Veschambre, M., Nicollet, C., Provost, A. (1996). Electron microprobe dating of monazite. *Chemical Geology*, 131, 37-53.
- Montel, J. M., Veschambre, M., Nicollet, C. (1994). Datation de la monazite à la microsonde électronique. *Comptes Rendus de l'Academie des Sciences de Paris*, 318, série II, 1984-1495.
- Moraes, R., Brown, M., Fuck, R. A., Camargo, M. A., Lima, T. M. (2002). Characterization and P-T evolution of melt-bearing ultrahigh-temperature granulite: an exemple from Anapolis-Ituaçu Complex of the Brasilia fold belt, Brazil. *Journal of Petrology*, 13, 1673-1705.
- Morse, S. A., Talley, J. H. (1971). Sapphirine reactions in deepseated granulites near Wilson Lake, central Labrador, Canada. *Earth and Planetary Science Letters*, 10, 325-328.

- Motoyoshi, Y., Hensen, B. J. (2001). F-rich phlogopite stability in ultra-high-temperature metapelites from Napier Complex, East Antarctica. *The American Mineralogist*, 86, 1404-1413.
- Mougeot, R. (1996). Étude de la limite archéen-protérozoïque et des mineralisations Au, \pm U associées: exemples des régions de Jacobina (Etat de Bahia, Brésil) et de Carajás (Etat de Pará, Brésil). Thèse (Doctorat). Montpellier: Université Montpellier II.
- Nasipuri, P., Bhattacharya, A., Das, S. (2009). Metamorphic reactions in dry and aluminous granulites: a Perple_X P-T pseudosection analysis of the influence of effective reaction volume. *Contributions to Mineralogy and Petrology*, 157, 301-311.
- Nicollet, C. (1990). Crustal evolution of the granulites of Madagascar. In: D. Vielzeuf, P. H. Vidal (Eds.), *Granulites and crustal evolution*, 291-310. Clermont Ferrand: Springer-Verlag.
- Oliveira, E. P., McNaughton, N. J., Armstrong, R. (2010). Mesoarchaean to Palaeoproterozoic growth of the northern segment of the Itabuna-Salvador Curaçá-orogen, São Francisco craton, Brazil. *Geological Society*, 338, 263-286.
- Ouzegane, K., Boumaza, S. (1996). An example of ultrahigh-temperature metamorphism: orthopyroxene-sillimanite-garnet, sapphirine-quartz and spinel-quartz parageneses in Al-Mg granulites from Hihaou, In Ouzzal, Hogar. *Journal of Metamorphic Geology*, 14, 693-708.
- Perchuk, L. L. (2011). Local mineral equilibria and P-T paths: Fundamental principles and applications to high-grade metamorphic terranes. *Geological Society of America*, 207, 61-84.
- Perchuk, L. L., Lavrent'eva, I. V. (1983). Experimental investigation of exchange equilibria in the system cordierite-garnet-biotite. In: S. K. Saxena (Ed.), *Advances in physical geochemistry*, 1-60. New York: Springer-Verlag.
- Peucat, J. J., Barbosa, J. S. F., Pinho, I. C. A., Paquette, J. L., Martin, H., Fanning, C. M., Menezes Leal, A. B., Cruz, S. P. C. (2011). Geochronology of granulites from the south Itabuna-Salvador-Curaçá Block, São Francisco Craton (Brazil): Nd isotopes and U-Pb zircon ages. *Journal of South American Earth Sciences*, 31, 397-413.
- Peucat, J. J., Mascarenhas, J. F., Barbosa, J. S. F., Souza, S. L., Marinho, M. M., Fanning, C. M., Leite, C. M. M. (2002). 3.3 Ga SHRIMP U-Pb zircon age of a felsic metavolcanic rock from the Mundo Novo Greenstone Belt in the São Francisco Craton, Bahia (NE, Brazil). *Journal of South American Earth Sciences*, 15, 363-373.
- Pinho, I. A. (2005). *Geologia dos metatonalitos/metatrondhjemitos e dos granulitos básicos das regiões de Camamu-Ubaitaba-Itabuna, Bahia*. Tese (Doutorado). Salvador: Instituto de Geociências – UFBA.
- Raith, M., Karmakar, S., Brown, M. (1997). Ultrahigh-temperature metamorphism and multi-stage decompressional evolution of sapphirine granulites from the Palni Hill Rangers, Southern India. *Journal of Metamorphic Geology*, 15, 379-399.
- Reche, J., Martinez, F. J. (1996). GPT: an Excel spreadsheet for thermobarometric calculations in metapelitic rocks. *Computers & Geosciences*, 22, 775-784.
- Rios, D. C. (2002). *Granitogenese no núcleo Serrinha, Bahia, Brasil: geocronologia e litogeochimica*. Tese (Doutorado). Salvador: Instituto de Geociências – UFBA.
- Santos Pinto, M. A. (1996). *Le recyclage de la croûte continentale archéenne: exemple du bloc du Gavião - Bahia, Brésil*. Thèse (Doctorat). Rennes: Université de Rennes I.
- Schobbenhaus, C., Campos, D. A., Derge, G. R., Asmus, H. E. (1984). *Geologia do Brasil: texto explicativo do Mapa Geológico do Brasil e da área oceânica adjacente, incluindo depósitos minerais*, 501 p. Brasília: Departamento Nacional da Produção Mineral.
- Seixas, S. R. M. (1993). *Estudo fotogeológico, petrográfico e petroquímico das rochas granulíticas da área de Almadina no Estado da Bahia*. Dissertação (Mestrado). Salvador: Instituto de Geociências – UFBA.
- Sen, S. K., Bhattacharya, A. (1984). An orthopyroxene-garnet thermometer and its applications to the Madras charnockites. *Contributions to Mineralogy and Petrology*, 68, 64-71.
- Sengupta, P., Dasgupta, S., Bhattacharya, P. K., Fukuoka, M., Chakraborti, S., Bhowmick, S. (1990). Petrotectonic imprints in sapphirine granulites from Anantagiri, Eastern Ghats, India and their implications. *Journal of Petrology*, 31, 971-996.
- Silva, L. C. (1991). *Caracterização microestrutural, geoquímica e petrogênese dos terrenos de alto grau das Folhas de Itabuna-Ibicarai, Salvador*, 230 p. Rio de Janeiro: CPRM (Publicação Especial).
- Silva, L. C., Armstrong, R., Delgado, I. M., Pimentel, M., Arcanjo, J. B., Melo, R. C., Teixeira, L. R., Jost, H., Cardoso Filho, J. M., Pereira, L. H. M. (2002). Reavaliação da evolução geológica em terrenos precambrianos brasileiros com base em novos dados U-Pb SHRIMP, Parte I: limite centro-oriental do craton do São Francisco na Bahia. *Revista Brasileira de Geociências*, 32(4), 501-512.
- Silva, M. G. (1992). Evidências isotópicas e geocronológicas de um fenômeno de acréscimo crustal transamazônico no Cráton do São Francisco, Estado da Bahia. *XXXVII Congresso Brasileiro de Geologia, São Paulo, Brazil*, v. 2, 181-182.

- Silva, M. G. (1996). Sequências Metasedimentares, Vulcanosedimentares e Greenstone Belts do Arqueano e Proterozoico Inferior. In: J. S. F Barbosa, J. M. L. Dominguez (Eds.), *Geologia da Bahia: Texto Explicativo para o Mapa Geológico ao Milionésimo*, 85-102. SICM/SGM. (Publicação Especial).
- Souza-Oliveira, J. S., Peucat, J. J., Barbosa, J. S. F., Corrêa-Gomes, L. C., Cruz, S. C. P., Menezes Leal, A. B., Paquette, J. L. (2014). Lithogeochemistry and geochronology of the subalkaline felsic plutonism that marks the end of the Paleoproterozoic orogeny in the Salvador–Esplanada belt, São Francisco craton (Salvador, state of Bahia, Brazil). *Brazilian Journal of Geology*, 44(2), 221-234.
- Teixeira, W., Carneiro, M. A., Noce, C. M., Machado, N., Sato, K., Taylor, P. N. (1996). Pb, Sr and Nd isotopic constraints on the Archean evolution of gneissic-granitoid complexes in the southern São Francisco Craton, Brazil. *Precambrian Research*, 78(1-3), 151-164.
- Thompson, A. B. (1976). Mineral reactions in pelitic rocks: I Prediction of P-T-X (Fe, Mg) phase relations, II Calculation of some P-T-X (Fe, Mg) phase relations. *American Journal of Science*, 276, 401-454.
- Tsunogae, T., Van Reenen, D. D. (2011). High-pressure and ultrahigh-temperature granulite-facies metamorphism of Precambrian high-grade terranes: case study of the Limpopo Complex. *Geological Society of America*, 207, 107-124.
- Ulmer, P. (1993). *Calculation of various Mineral – Norms*. Program NORM: Version 4.0.
- Vielzeuf, D., Holloway, J. R. (1988). Experimental determination of the fluid-absent melting reactions in the pelitic system. Consequences for crustal differentiation. *Contributions to Mineralogy and Petrology*, 98, 257-276.
- Waters, D. J. (1991). Hercynite-quartz granulites: phase relations and implications for crustal processes. *European Journal of Mineralogy*, 3, 367-386.
- Whitney, D. L., Evans, B. W. (2010). Abbreviations for names of rock-forming minerals. *The American Mineralogist*, 95, 185-187.